J Fusion Energ (2014) 33:588–593
DOI 10.1007/s10894-014-9715-4

ORIGINAL RESEARCH

Thermal Design of High-Power DC Reactor for ITER Poloidal Field Converter

Chuan Li · Zhiquan Song · P. Fu · Ming Zhang · Xiuqing Zhang · Kexun Yu

Published online: 22 May 2014

Abstract This paper presents an alternative computationally efficient approach to the thermal design of high-power DC reactor which is applied to ITER poloidal field converter module. The proposed approach takes full advantages of the property of time-saving from heat transfer theory and high accuracy from 3-D finite-element analysis, focusing on the predictions of the temperature rise and pressure loss of circulating water. Thermal measurements from two prototypes test show a good agreement with the predictions, which proves the high efficiency and accuracy of the proposed approach in the design of hundred-kilowatt-class thermal power DC reactor.

Keywords ITER · Poloidal field converter · DC reactor · Thermal analysis

Disclaimer: The view and opinion expressed herein does not necessarily reflect those of the ITER organization.

C. Li · M. Zhang (✉) · K. Yu
State Key Laboratory of Advanced Electromagnetic Engineering and Technology, Huazhong University of Science and Technology, Room 316, Bldg East 15, East Campus, 1037 Luoyu Rd, Wuhan 430074, People's Republic of China
e-mail: zhangming_hust@126.com

C. Li · M. Zhang · K. Yu
School of Electrical and Electronic Engineering, Huazhong University of Science and Technology, Wuhan 430074, People's Republic of China

Z. Song · P. Fu · X. Zhang
Institute of Plasma Physics, Chinese Academy of Science, Hefei 230031, People's Republic of China

Introduction

International Thermonuclear Experimental Reactor (ITER), which is an international nuclear fusion project, is aimed to demonstrate the feasibility of realizing the commercial value of fusion energy. The poloidal field (PF) converter module, as an important part of ITER equipment, plays an essential role in the plasma shape and position control in vertical and horizontal direction [1–3]. In the course of PF converter module normal operation, circulating current and ripple current may occur between two converter module units [4], which poses a severe threat to the normal operation of the converter module and needs to be suppressed. More seriously, fault current up to 175 kA-class may exhibit when the main circuit happens before-reactor short-circuit [3]. Furthermore, the quick increase rate of the fault current and the concomitant induced voltage may cause irreparable damage to the relevant equipment. As a significant part to restrain circulating current, ripple current and limit the DC short-circuit current and its increase rate, a reliable type of DC reactor is therefore an essential part of the design process, which is proposed in this paper. Due to the long-term operation under large rated direct current 27.5 kA, the temperature of winds will rise rapidly without proper disposition of the concomitant high heat power, which can be up to several hundred kilowatts. Therefore, accurate prediction of the temperature is of significant importance.

Several methods commonly applied in thermal analysis are listed as follows. (1) Analytical equivalent thermal circuit method, which provides a quick and succinct solution but usually needs initial information of the model and it is arduous to reach the required accuracy [5]; (2) numerical computational fluid dynamics. Due to the property of time consuming, its use is limited, although the

result is accurate [6]; (3) thermal finite-element (FE) analysis (FEAs) [7], which has more accurate predictions with requiring detailed parameters in modeling progress. In general, an FE-based model needs the geometrical model of a device, together with the material properties, boundary conditions and excitations [8]. In this paper, a hybrid approach to predict the thermal property is proposed based on the use of heat transfer theory combining with 3-D thermal FEAs and be verified further by prototype test. The use of heat transfer theory significantly simplifies the model definition and consequently reduces the solution time to get a preliminary design. In addition, the further verification of 3-D thermal FEA can ensure the required accuracy of the promoted design. In general, the proposed approach takes full advantages of the property of time-saving from heat transfer theory and high accuracy from 3-D thermal FEA.

In this paper, the assembly and technical parameters of the prototype reactor are introduced. Based on the analysis methods, including thermal calculation methods and 3-D thermal FEA, the temperature rise and pressure loss of circulating water are analyzed and predicted. With the experimental results from prototype test, the high efficiency and accuracy of the hybrid approach are proved.

Full Prototype Reactor

From the market research report, copper is heavier and more expensive in comparison with aluminum, although it has better performance in electrical conductivity. Therefore, aluminum is the chosen conductive material for the prototype reactor. The specific model is aluminum 6063-O. In general, the safe current carrying of aluminum wire with water-cooling should not exceed 5 A/mm^2, so the total equivalent conductive area should not be less than 5,500 mm^2 which cannot be found in a single wire from the market research results. Finally, five tubes are connected in parallel to achieve the required large cross-section area. The tube is a square cross-section hollow conductor with dimensions of 50 mm × 40 mm, a 25 mm center hole for cooling water, and a fillet radius of 3 mm. Therefore, the current density equals to approximately 3.72 A/mm^2, which meets the requirements.

The full prototype consists of two identical parts in series. Each part includes five tubes with the same dimension with the average diameter of 1.21 m. The inductance is 193-μH at a ripple current with the frequency of 300 Hz. The input and output terminals are located on opposite side with respect to the reactor for ease of the busbar assembly. The aluminum tubes are reinforced by multilayer high-strength e-glass ribbons and the full prototype is cast by epoxy resin with vacuum pressure impregnation (VPI) technology. The overall structure is shown in Fig. 1.

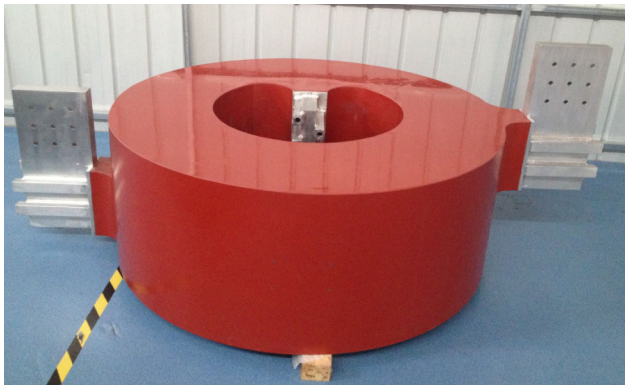

Fig. 1 The prototype reactor with the average diameter of 1.21 m and the inductance of 193-μH at 300 Hz

Analysis Method and Measurement Setup

Heat Transfer Theory Analysis

The resistance also depends on the temperature

$$\rho_{Al} = \rho_{Al(10^{\circ}C)}(1 + \Delta T \alpha_{Al}) \quad (1)$$

where $\rho_{Al(10\ ^{\circ}C)}$ is the resistivity of aluminum at 10 °C, ΔT is the temperature difference to 10 °C, and α_{Al} is the temperature coefficient of resistivity. The temperature coefficient of the resistivity for aluminum is $\alpha_{Al} = 4.03 \times 10^{-3}$ 1/K [9]. Since the actual resistivity of aluminum alloy is a few percent higher than that of pure aluminum, thus, the material data for the analysis is equal to 2.96×10^{-8} Ωm at 10 °C from experimental measurement. Moreover, the initial temperature of circulating water is 32 °C and the temperature rise is required to not exceed 20 °C, so the average value (i.e. 42 °C) is assumed to be the temperature of tube in the analysis process, which means the ΔT is 32 °C.

According to the sectional dimensions mentioned above, the length and sectional area of a parallel coil are 32 m and 1,500 mm^2, respectively. The electric resistivity of aluminum alloy 6063-O at 42 °C is approximately equal to 713 μΩ based on the formula (1). On account of the prototype consists of two identical parts in series, which includes five tubes in parallel, the total resistance of prototype is about 285 μΩ (i.e. two fifths of the resistance of one tube). Therefore, the total heat power at rated direct current 27.5 kA is about 215.5 kW.

To approximately calculate the heat power and required circulating water flow, a number of assumptions have been proposed. Firstly, the ripple current is neglected and only

direct current flows through the tubes. Secondly, the current distribution inside DC reactor is uniform. Thirdly, due to the existence of resin casting, the coil is thermal insulated from the external, and all the heat is transferred by flowing circulating water. Based on the assumptions described previously, the temperature rise between inlet and outlet of water can be estimated by formula (2). Formula (3) shows the relationship between flow and fluid velocity.

$$P = CM\Delta T \tag{2}$$

$$M = m\rho\pi(d/2)^2 V \tag{3}$$

where

P total heat power (in kW);
C fluid specific heat capacity [kJ/(kg °C)];
M cooling water flow [kg/s];
ΔT difference between inlet and outlet temperatures (in °C);
m the number of tubes of a prototype, $m = 10$ for the full prototype;
ρ density of water (kg/m^3);
d the diameter of water passage, $d = 0.025$ m;
V fluid velocity (in m/s)

In addition, the preliminary estimates of the pressure loss through the aluminum tube can be obtained by the formula (4)–(7) as follows [10].

$$R_e = Vd/v \tag{4}$$

$$h_f = \lambda l V^2/2dg \tag{5}$$

$$h_j = n\xi V^2/2g \tag{6}$$

$$\Delta P = (h_f + h_j)\rho g \tag{7}$$

where

R_e Reynolds number;
V fluid velocity (in m/s);
D the diameter of water passage, $d = 0.025$ m
v kinematic viscosity of water, $v = 0.638 \times 10^{-6}$ m^2/s at 42 °C;
h_f frictional water loss (in m);
λ path loss coefficient;
l the length of a tube (in m);
g gravitational attraction force (in m/s^2);
h_j total partial loss of a tube (in m);
n the layers of a tube, $n \approx 8$, here;
ζ partial loss coefficient;
ΔP difference between inlet and outlet pressure (kPa);
ρ density of water (kg/m^3)

According to relationships described previously, the curves of temperature rise and water pressure loss versus the fluid velocity are shown in Fig. 2.

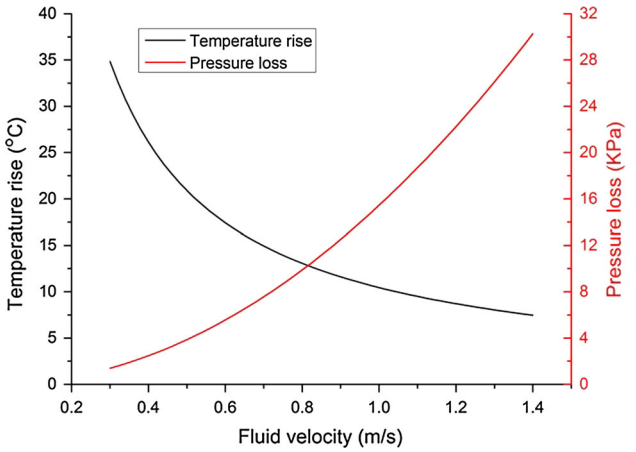

Fig. 2 The curves of temperature rise and water pressure loss versus the fluid velocity

Table 1 Part of parameters of 3-D thermal FEA simulation

Parameters	Values
Water temperature at inlet	32 °C
Water velocity	1.0 m/s
Water pressure at outlet	1.013×10^5 Pa
Electrical conductivity of aluminum (at 42 °C)	2.99×10^7 S/m
The current of a tube	5.5 kA

Figure 2 shows that, to ensure the temperature rise do not exceed 20 °C, the fluid velocity should not be less than 0.52 m/s. Considering the economic cost and the requirements for water flow of other relevant equipments of PF converter, the fluid velocity is set to be 1.0 m/s. Correspondingly, the predicted value of the temperature rise and the water pressure loss are 10.5 °C and 15.4 kPa, respectively. The total circulating water flow for the whole reactor is 17.6 m^3/h.

Finite Element Analysis (FEA)

The thermal analysis of prototype and circulating water is a fluid–solid coupling problem. Due to the difficulty in acquiring analytic solutions, 3-D thermal FEA is adopted to get the high-accuracy results. By the module of Workbench CFX, the temperature distribution of prototype and pressure distribution of circulating water can be worked out. The material properties, boundary conditions and excitations of FE model are partly shown in Table 1.

Figure 3 shows the temperature distribution of a single coil with circulating water. The maximum temperature of coil is about 47.74 °C at the insider corner as a result of partly nonuniform current distribution. So the maximum temperature difference between water and coil is 15.74 °C, while average water temperature rise is 10.9 °C. Since the

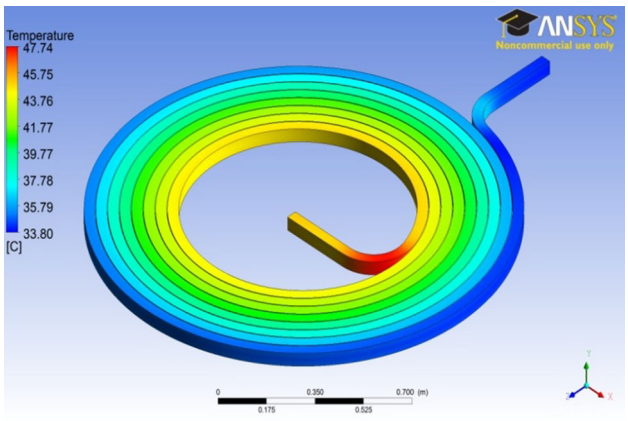

Fig. 3 Temperature of the aluminum tube

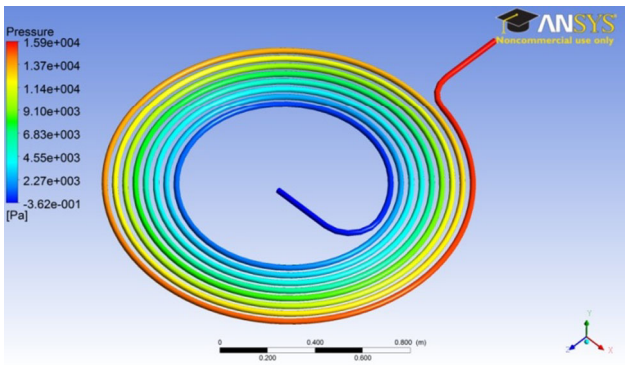

Fig. 4 Water pressure distribution of a single coil

relative pressure is set to be 0 Pa in the FE-based model, the pressure loss of a tube is about 15.9 kPa, as shown in Fig. 4.

Measurement Setup

In October 2013, the direct current testing platform of the Institute of Plasma Physics, Chinese Academy of Sciences (ASIPP) has passed commissioning of 250 kA short-circuit current and it can provide a stable current range of 0–120 kA. By means of closed-loop control, the DC current 27.5 kA of thermal stability test is realized.

Several current sensors are used to measure the circuit current. The temperature within the prototype assembly is monitored in a number of points, including the surfaces of reactor, busbar, water container, and support device. Data acquisition and recording are based on the temperature logger. The thermal imager is used to detect the partial hot spots at any time. The ambient temperature is detected by mercurial thermometer with hanging in the air. The more detailed information is shown in Table 2. Before being used, all above measuring instruments have been calibrated by relevant departments of metrology institutes.

Table 2 The information of the equipments of the test system

Equipment	Model	Range	Preciseness
DC testing platform	–	0–120 kA (stable state)	–
Current sensor	LKCO-130	0–130 kA	0.1 %
Thermal resistor	pt100	−200 to +500 °C	±(0.15 + 0.002 t)
Temperature logger	XSR70A/Y1-32RS2V0USB	32 channels	±0.2 % FS.
Thermal imager	Fluke Ti10	−20 to +250 °C	±2 °C or 2 %
Thermometer	Mercurial thermometer	0 to +100 °C	Minimum graduation 1 °C

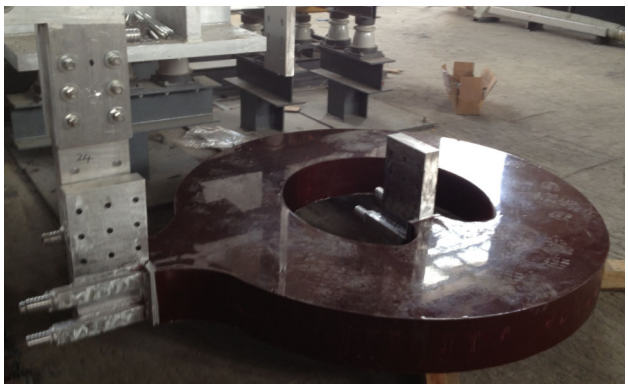

Fig. 5 A small prototype for small step-by-step current test

Experimental Results

A Small Prototype Test

In order to reduce the risk and verify the feasibility of the design, a small prototype has been fabricated by China industry and tested at ASIPP. As shown in Fig. 5, the small prototype is composed of three tubes in parallel. With the purpose of providing a reference to the manufacture of full prototype, the current carrying should keep in compliance with the design value (i.e. 3.72 A/mm^2). Therefore, the rated current should be 16.5 kA. Correspondingly, the water flow is maintained at 5.3 m^3/h.

Test current increases step by step from 6 to 21 kA. The temperature variation history of cooling water versus time is shown in Fig. 6, visually revealing the temperature-rise process. The initial temperature of circulating water is 28.2 °C and the corresponding temperature rises of 6, 12, 16.5 and 21 kA are 1.3, 5.7, 10.8 and 17.7 °C, respectively. The water pressure loss is 16.5 kPa, including the loss in

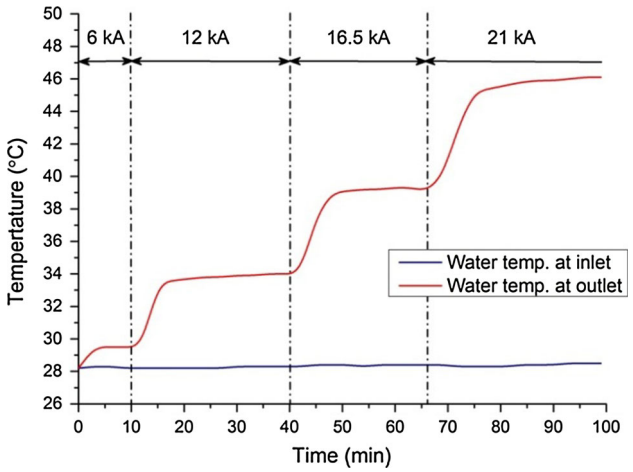

Fig. 6 The temperature rise test of a small prototype

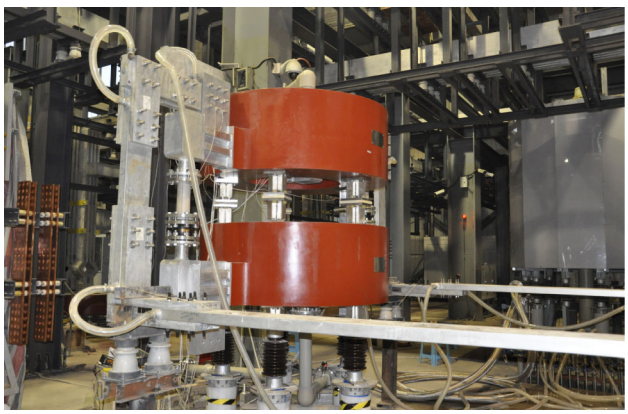

Fig. 7 Temperature rise test for full prototype

external water pipes. It shows a good agreement with the predictions.

A Full Prototype Test

The accomplishment and the test results of small prototype show the feasibility of the promoted design. Then a full prototype is fabricated, and tested on the direct current platform of ASIPP, which is shown in Fig. 7.

The test equipment is as shown in Table 2. The wave of test current is shown in Fig. 8, with the rms of 27.73 kA. The experimental circulating water flow is 18 m^3/h.

Figure 9 depicts the temperature variation of circulating water. At the beginning of stage b, the damping of water temperature at inlet is on account of the starting of fan, which is used to cool the circulating water. The water temperature at outlet varies with the water temperature at inlet. However, the temperature rise keeps at a stable value about 10.9 °C. The thermal imager is used to detect the partial hot spots, and the data from Fig. 10 shows that the surface temperature is maintained at a low level. In

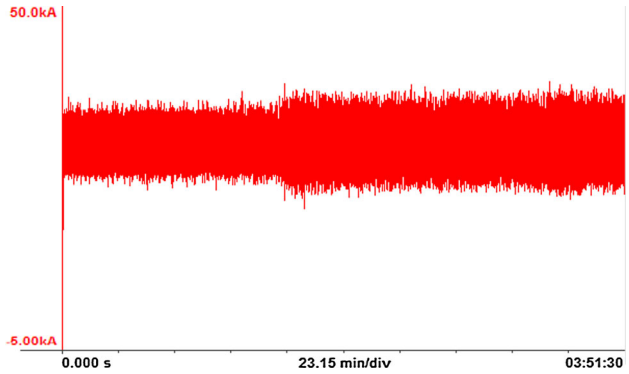

Fig. 8 The test current with the rms of 27.73 kA

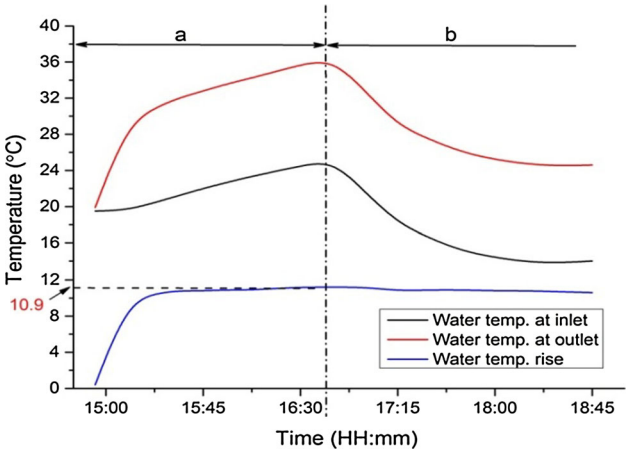

Fig. 9 The temperature rise test of a full prototype

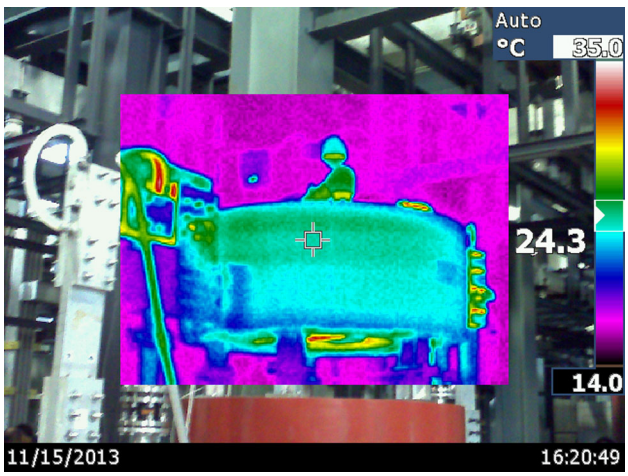

Fig. 10 Thermal image of a full prototype

addition, the total water pressure loss is 45 kPa, which mainly includes the pressure loss in the tube and external vertical water pipes. With the neglect of the latter pressure loss, the average pressure loss in a tube is 22.5 kPa, which is also close to the prediction.

Table 3 Contrast in the results from various methods

Parameters	Theoretical calculations	FEA simulations	Small prototype	Full prototype
Water flow (m^3/h)	17.6	17.6	5.3	18.0
Temperature rise (°C)	10.5	10.9	10.8	10.9
Pressure loss of a single tube (kPa)	15.4	15.9	16.5	22.5

Summary and Conclusion

The experimental results are compared with the predictions from the other methods in Table 3. It is obvious that the results correspond very well in the estimations of temperature rise and pressure loss. The pressure loss of a single tube of full prototype is a few percent higher than that of the small prototype, which is owing to the pressure loss in the vertical water pipes. As shown in Fig. 7, the vertical water pipes are used to connect the circulating water of the upper and lower reactor. In general, the contrast proves that a time-saving and high accurate design of thermal stability can be achieved by using the promoted method.

This paper fulfilled the thermal stability design of a high-power reactor, focusing on the analyses of cooling water, particularly in the predictions of temperature rise and pressure loss. Based on the promoted structure, a small prototype is fabricated and tested, with the aim to verify the theoretical predictions and provide a reference to the design of full prototype. The measurements from full prototype show a good agreement with the results from various methods, which further demonstrates the high efficiency and accuracy of the hybrid approach and the high reliability of the promoted design.

Acknowledgments The authors would like to express gratitude to Ministry of Science and Technology of China for the foundation and staff of ASIPP for helpful discussions and suggestions.

References

1. P. Fu, G. Gao et al., Preliminary design of the poloidal field AC/DC converter system for the ITER coil power supply. Fusion Sci. Technol. **64**(4), 741–747 (2013)
2. P.L. Mondino et al., ITER R&D: auxiliary systems: coil power supply components. Fusion Eng. Des. **55**, 325–330 (2001)
3. P. Fu, G. Gao et al., Review and analysis of the ac/dc converter of ITER coil power supply, in *Proceedings of Applied Power Electronics Conference, IEEE*, Palm Spring, CA, USA, pp. 1810–1816 (2010)
4. H. Yuan, P. Fu et al., On the circulating current control of ITER poloidal field converter. J. Fusion Energ. **33**(3), 269–274 (2010)
5. D.A. Staton, A. Cavagnino, Convection heat transfer and flow calculations suitable for electric machines thermal models. IEEE Trans. Ind. Electron. **55**(10), 3509–3516 (2008)
6. F. Marignetti, V.D. Colli, Y. Coia, Design of axial flux PM synchronous machines through 3-D coupled electromagnetic thermal and fluid-dynamical finite-element analysis. IEEE Trans. Ind. Electron. **55**(10), 3591–3601 (2008)
7. A. Boglietti, A. Cavagnino, D. Staton, M. Shanel, M. Mueller, C. Mejuto, Evolution and modern approaches for thermal analysis of electrical machines. IEEE Trans. Ind. Electron. **56**(3), 871–882 (2009)
8. R. Wrobel, P. Mellor, Thermal design of high-energy-density wound components. IEEE Trans. Ind. Electron. **58**(9), 4096–4104 (2011)
9. W. Zhutang, T. Rongzhang, *Aluminum Alloy and its Manufacturing Handbook* (Central South University Press, Changsha, 2007)
10. Z. Hanzhong, *Engineering Fluid Mechanics* (Huazhong University of Science & Technology Press, Wuhan, 2011)